Matters Arising

Cell

Autophagic Components Contribute to Hypersensitive Cell Death in *Arabidopsis*

Daniel Hofius,[1] Torsten Schultz-Larsen,[1,3] Jan Joensen,[1] Dimitrios I. Tsitsigiannis,[2,4] Nikolaj H.T. Petersen,[1,5] Ole Mattsson,[1] Lise Bolt Jørgensen,[1] Jonathan D.G. Jones,[2] John Mundy,[1] and Morten Petersen[1,*]

[1]Department of Biology, Copenhagen Biocenter, University of Copenhagen, 2200 Copenhagen, Denmark
[2]The Sainsbury Laboratory, John Innes Centre, Norwich Research Park, Norwich NR4 7UH, UK
[3]Present address: The Sainsbury Laboratory, John Innes Centre, Norwich Research Park, Norwich NR4 7UH, UK
[4]Present address: Department of Crop Science, Agricultural University of Athens, 118 55 Athens, Greece
[5]Present address: Danish Cancer Society, Department of Apoptosis, Institute of Cancer Biology, 2100 Copenhagen, Denmark
*Correspondence: shutko@bio.ku.dk
DOI 10.1016/j.cell.2009.02.036

SUMMARY

Autophagy has been implicated as a prosurvival mechanism to restrict programmed cell death (PCD) associated with the pathogen-triggered hypersensitive response (HR) during plant innate immunity. This model is based on the observation that HR lesions spread in plants with reduced autophagy gene expression. Here, we examined receptor-mediated HR PCD responses in autophagy-deficient *Arabidopsis* knockout mutants (*atg*), and show that infection-induced lesions are contained in *atg* mutants. We also provide evidence that HR cell death initiated via Toll/Interleukin-1 (TIR)-type immune receptors through the defense regulator EDS1 is suppressed in *atg* mutants. Furthermore, we demonstrate that PCD triggered by coiled-coil (CC)-type immune receptors via NDR1 is either autophagy-independent or engages autophagic components with cathepsins and other unidentified cell death mediators. Thus, autophagic cell death contributes to HR PCD and can function in parallel with other prodeath pathways.

INTRODUCTION

Plants have evolved a multilayered immune system to recognize and respond to invading pathogens. The first layer includes pattern recognition receptors that detect conserved microbial associated molecular patterns and initiate an immune response (Jones and Dangl, 2006). Another layer uses resistance (R) proteins whose activation triggers a rapid defense response that often includes a localized programmed cell death (PCD) reaction known as the hypersensitive response (HR) (Nimchuk et al., 2003). The most prevalent type of plant R proteins belongs to the nucleotide binding site (NB)-leucine-rich repeat (LRR) class that can be further separated into Toll/Interleukin-1 receptor (TIR)- or coiled-coil (CC)-NB-LRR R proteins (Dangl and Jones, 2001).

To overcome the first defense layer, successful pathogens deliver various virulence determinants, termed effectors, into plant cells. These effectors modify host proteins and manipulate the host cellular machinery to suppress immune responses and enhance virulence (Bent and Mackey, 2007). Gram-negative phytopathogenic bacteria, such as *Pseudomonas syringae*, use a type III secretion system (T3SS) for the export and translocation of effectors into host cells. Infection and multiplication of bacteria in the leaf interior can lead to disease-associated cell death, which typically appears several days after infection (Abramovitch et al., 2006). However, if type III effector functions on host targets are perceived by specific alleles of NB-LRR genes, they act as avirulence factors (Avr proteins), and elicit HR PCD within hours after pathogen attack (Lam, 2004).

Signaling components of *R*-gene mediated HR have been identified in genetic screens for loss of resistance to bacterial and oomycete pathogens in *Arabidopsis*. These analyses revealed that *ENHANCED DISEASE SUSCEPTIBILITY* 1 (*EDS1*) and *NON RACE-SPECIFIC DISEASE RESISTANCE* (*NDR1*) are required for the function of different *R* genes. Loss of *EDS1* function suppresses signals generated by TIR-NB-LRR R proteins, whereas *ndr1* mutants are compromised in resistance conditioned by CC-NB-LRR R proteins (Aarts et al., 1998).

In contrast to the well-documented signaling pathways associated with HR induction, little is known about how HR cell death is executed, or whether plants share conserved death mechanisms with metazoans (Hofius et al., 2007). The best described form of PCD in animals is apoptosis, but plants apparently lack apoptotic regulatory genes including cysteine proteases called caspases (Lam et al., 2001). Nonetheless, caspase-like activities have been detected during HR and disease-related cell death which could be assigned to different types of proteases (Woltering, 2004; Vercammen et al., 2007). Among them, the vacuolar processing enzyme (VPE) was shown to exhibit caspase-1 activity and to act as an executor of *Tobacco mosaic virus* (TMV)-triggered PCD in tobacco (Hatsugai et al., 2004). Additionally, the protease cathepsin B has been implicated in pathogen-induced PCD (Gilroy et al., 2007). Cathepsins generally function in lysosomal catabolic processes and are

involved in apoptotic and necrotic types of PCD (Guicciardi et al., 2004).

Another, nonapoptotic form of animal PCD involves autophagy (Edinger and Thompson, 2004), an ancient vesicular mechanism for digestion of cell contents in eukaryotes (Mizushima, 2007). A central feature of autophagy is the formation of double membrane vesicles, named autophagosomes, that engulf and deliver portions of the cytoplasm to the vacuole/lysosome for degradation (Levine and Klionsky, 2004; Mizushima, 2007). Autophagosome initiation and completion are mediated by autophagy-related proteins (ATGs) and require two ubiquitin-like conjugation systems to produce ATG12-ATG5 and ATG8-phosphatidylethanolamine (ATG8-PE) conjugates. ATG8-PE conjugation involves the cysteine proteinase ATG4 and the E1-like protein ATG7, and lipidated ATG8 is linked to and translocated with autophagosomes to the vacuole (Geng and Klionsky, 2008). Therefore, conversion from soluble to lipid bound ATG8, as well as subcellular localization of green fluorescent protein (GFP) fused protein, have been used to monitor the occurrence of autophagy (Klionsky et al., 2008). Plants have a complement of autophagy proteins, and loss-of-function mutations in ATG genes such as ATG9, ATG7, ATG5, and ATG4a/b indicate that autophagy is central to plant source-sink relations and senescence (Thompson et al., 2005; Bassham et al., 2006).

Autophagy is also implicated in animal innate immunity, and as an alternative death pathway which may be invoked during development (Gutierrez et al., 2004; Nakagawa et al., 2004; Berry and Baehrecke, 2007). However, no genetic evidence has yet been provided in plants that autophagy has a prodeath function in either developmental or pathogen-inducible PCD. Instead, two reports indicate that autophagy is required to limit the spread of HR related cell death. Liu et al. (2005) used virus-induced gene silencing to downregulate autophagy genes including *BECLIN1/ATG6* and *ATG7* in *Nicotiana benthamiana* expressing the *N* resistance gene. TMV infection of silenced plants triggered *N*-mediated HR cell death that extended to uninfected tissue and to leaves distant from the infection site in which viral RNA was undetectable (Liu et al., 2005). These data suggested that systemic spread of prodeath signal(s) was no longer limited in autophagy-deficient cells. The conclusion that autophagy negatively regulates PCD in plant innate immunity is apparently supported by a recent finding in another host-pathogen system. In *Arabidopsis*, *BECLIN1/ATG6* was shown to limit HR PCD conditioned by the RPM1 immune receptor upon local infections with avirulent *Pseudomonas syringae* pv. tomato (*Pto)* strain DC3000 harboring the avirulence gene *AvrRpm1* (Patel and Dinesh-Kumar, 2008). However, due to the essential role of Beclin1/ATG6 in pollen germination and plant development (Harrison-Lowe and Olsen, 2008), Patel and Dinesh-Kumar (2008) were unable to obtain homozygous knockout mutants and therefore used antisense plants with various developmental abnormalities. Thus, the role of autophagy in plant innate immunity has so far only been studied by knock down approaches in tobacco and *Arabidopsis*.

Using autophagy-deficient *Arabidopsis* knockout mutants, we provide genetic evidence that TIR-class NB-LRR receptors can activate EDS1-dependent, autophagic cell death during HR execution. We also demonstrate that strong HR cell death triggered by the CC-type immune receptor RPM1 involves autophagy and other PCD types. In contrast, we show that HR cell death induced by another CC-NB-LRR class receptor, RPS2, activates NDR1-dependent but autophagy-independent cell death. Therefore, we provide examples of the contribution of autophagy components to cell death execution in plant innate immune responses.

RESULTS

Restricted HR Lesions in *Arabidopsis atg* Mutants

Arabidopsis is a genetically tractable plant model and autophagy-deficient mutants have been described that, unlike *BECLIN1/ATG6* antisense lines, are indistinguishable from wild-type plants when nutrients are not limited (Thompson et al., 2005). Therefore, we examined whether uncontrolled cell death could also be observed in *Arabidopsis* autophagy-deficient knockout mutants. First, we challenged the loss-of-function mutants *atg7* and *atg9* (Doelling et al., 2002; Thompson et al., 2005) with avirulent strains of *Pseudomonas syringae* pv. tomato (*Pto*) DC3000 harboring the avirulence genes *AvrRps4* or *AvrRpm1*. HR PCD elicited by *Pto* DC3000 (*AvrRps4*) requires the TIR-NB-LRR class *R* gene *RPS4*, whereas HR in response to *Pto* DC3000 (*AvrRpm1*) is conditioned by the CC-NB-LRR *R* gene *RPM1* (Aarts et al., 1998). Parts of leaves of *atg7*, *atg9* and wild-type Wassilewskija (Ws-0) were infected, and HR-associated symptom spread followed over several days. Surprisingly, no signs of death or tissue collapse were detectable in *atg7* and *atg9* beyond the primary HR lesion sites after infection, even after 15 days (see Figures S1A and S1B available with this article online). We also examined disease-associated cell death induced by virulent *Pto* DC3000. Again, lesions were contained and did not spread further than the initial infection site (Figure S1C).

Autophagy is induced by different pathogens in both animals and plants (Gutierrez et al., 2004; Liu et al., 2005). In *Arabidopsis*, autophagy genes are transcriptionally upregulated, but autophagic activity has not been demonstrated upon pathogen infections (Seay et al., 2006; Patel and Dinesh-Kumar, 2008). Therefore, we investigated whether autophagy was also associated with HR cell death in response to bacterial infection in *Arabidopsis*. To this end, we first used LysoTracker Green dye that stains acidic organelles such as autophagolysosomes to visualize possible autophagic activity (Liu et al., 2005). Cells examined before infection did not accumulate punctate structures that could indicate autophagic activity (Figure 1A). In contrast, we found that cells 3 hr after infection with *Pto* DC3000 (*AvrRpm1*) and 6 hr after infection with *Pto* DC3000 (*AvrRps4*) accumulated abundant autolysosomal-like structures (Figures 1A and S2A). The accumulation of these acidic organelles is likely to be caused by activation of *R* genes, because virulent infections with *Pto* DC3000 looked similar to cells examined before infection within this timeframe (Figure 1A). We then examined the occurrence of autophagy by assessing the behavior of ATG8 proteins during infection (Ichimura et al., 2004). ATG8 accumulation and modification, as indicated by the appearance of a faster migrating gel band, was detected 2 hr post *Pto* DC3000 (*AvrRpm1*) infection, and ATG8 processing increased to a maximum 6 hr after infection at which time *AvrRpm1* triggered host cell death is complete (Figure 1B) (Mackey et al., 2003). Processed forms of ATG8 started to

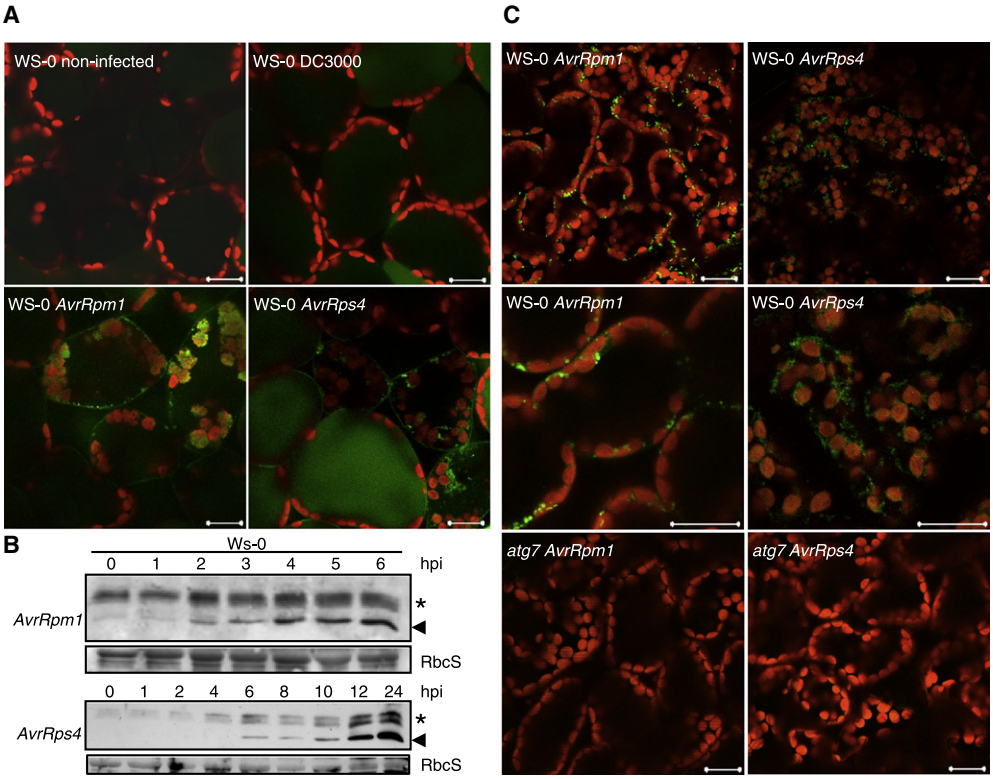

Figure 1. Autophagy Induction upon Avirulent Bacterial Infection

(A) LysoTracker Green (LTG) staining of autophagosomal-like structures in leaves of wild-type (Ws-0) plants upon infection with virulent *Pto* DC3000 or strains harboring avirulence factors *AvrRpm1* or *AvrRps4*. LTG-derived fluorescence was apparent in palisade parenchyma cells after 3 hr in *Pto* DC3000 (*AvrRpm1*) and 6 hr in *Pto* DC3000 (*AvrRps4*) infected Ws-0 leaves. Leaves challenged with virulent *Pto* DC3000 did not show LTG-specific signals during this time frame and were comparable to noninfected controls. Green channel images of LTG-derived fluorescence are superimposed with red autofluorescence of chloroplasts. Scale bars represent 20 μm.

(B) Immunoblot analysis of ATG8 accumulation and modification following avirulent bacterial infection. Total proteins were extracted at the indicated times points after infection with *Pto* DC3000 (*AvrRpm1*) or (*AvrRps4*), separated by SDS-PAGE, and probed on blots with anti-ATG8a antiserum. Unmodified ATG8 forms are indicated by asterisks and lipidated ATG8 forms are marked with an arrowhead. Crossreacting bands of the Rubisco large subunit (RbcS) served as loading controls.

(C) Confocal microscopy of transiently expressed GFP-ATG8 in wild-type (Ws-0) and autophagy-deficient *atg7* following infection with avirulent *Pto* DC3000 (*AvrRpm1* or *AvrRps4*). Images of indicated genotypes are representative of palisade parenchyma cells in leaves 3 hr (*AvrRpm1*) or 6 hr (*AvrRps4*) after infection. Green channel images of GFP-ATG8 derived fluorescence are superimposed with chlorophyll-derived red fluorescence of chloroplasts. Scale bars represent 20 μm.

accumulate 6 hr post *Pto* DC3000 (*AvrRps4*) infection and reached a maximum 24 hr post infection when cell death was completed (Figure 1B). Since *Arabidopsis* ATG8 associates with autophagosomal membranes after induction of autophagy (Yoshimoto et al., 2004), we additionally monitored autophagy activity with transiently expressed GFP-ATG8 fusion. GFP-derived fluorescence was not detectable in leaves before inoculation (data not shown), but occurred as punctate, autophagosomal-like structures throughout leaves 3 hr after infection with *Pto* DC3000 (*AvrRpm1*), and after 6 hr with *Pto* DC3000 (*AvrRps4*) (Figures 1C and S2B). GFP-like fluorescence was not detected in *atg7* (Figure 1C) or in nontransfected control plants (data not shown) upon infection with avirulent bacteria. Collectively, these data indicate that autophagy is induced upon avirulent bacterial infection in *Arabidopsis*, and that ATG7 and ATG9, in apparent contrast to BECLIN1/ATG6, are not required to restrict HR cell death.

Autophagic Components Are Necessary for RPS4- and RPP1-Mediated Cell Death

To assess whether autophagy induction affects PCD processes upon avirulent bacterial infection, we monitored cell death development in infected leaves of *atg7* and *atg9*. The effect of *Pto* DC3000 (*AvrRps4*)- or (*AvrRpm1*)-induced HR cell death was quantified using an electrolyte leakage assay (Mackey et al., 2003), as cell death causes release of electrolytes measured as changes in the conductance of a bath solution. These assays showed that *Pto* DC3000 (*AvrRps4*)-induced cell death caused an increase in conductance in Ws-0 by 10–12 hr (Figure 2A). However, this increase was significantly suppressed in the *atg7* and *atg9* mutants (Figure 2A). In contrast, inoculation of *atg7* and *atg9* mutants with *Pto* DC3000 (*AvrRpm1*) resulted in a minor but not significant reduction in electrolyte leakage compared to wild-type (Figure 2B).

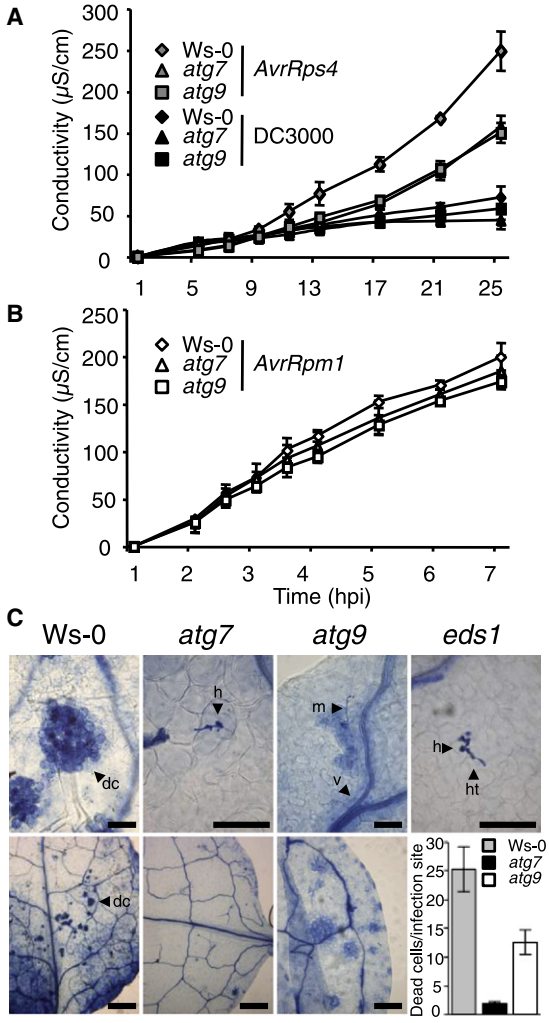

Figure 2. Suppression of *Pto* DC3000 (*AvrRps4*)- and Noco2-Mediated HR Cell Death in Autophagy-Deficient Mutants

(A and B) Ion leakage measurements of wild-type (Ws-0), *atg7* and *atg9* plants after inoculation with avirulent strains of *Pto* DC3000 expressing *AvrRps4* (A) or *AvrRpm1* (B). For comparison, ion leakage measurements of wild-type Ws-0, *atg7* or *atg9* infected with virulent *Pto* DC3000 are included (A). Mean and standard error (SE) were calculated from four disks per treatment, with three replicates within an experiment. Similar results were obtained in three independent experiments.

(C) Lactophenol-trypan blue staining of leaves from three-week-old Ws-0, *atg7*, *atg9,* and *eds1* seedlings infected with *H. arabidopsidis* race Noco2. Samples were stained 24 hr after infection. Dark blue staining detects dead mesophyll cells (dc). Scale bar in upper panel represent 100 μm, in lower panel 800 μm. The experiments were repeated three times with similar results. Insert (bottom right) shows number of dead cells (dc) per infection site for *atg7* and *atg9* in comparison to Ws-0. Error bars represent SE of the mean. Abbreviations are as follows: h, haustoria; ht, developing hyphal tip; m, mycelium; v, vascular tissue.

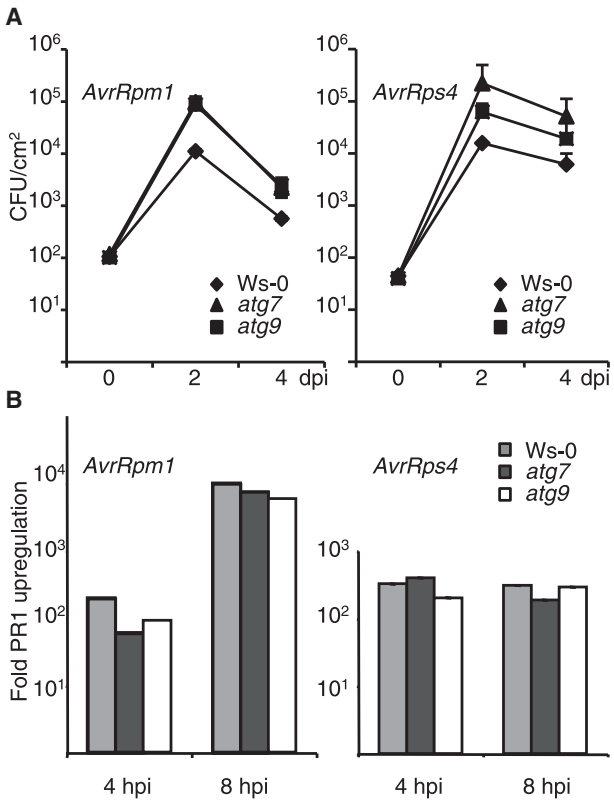

Figure 3. Contribution of Autophagy to Disease Resistance against Avirulent Bacteria

(A) Growth of avirulent *Pto* DC3000 expressing *AvrRpm1* or *AvrRps4* on wild-type Ws-0, *atg7* or *atg9*. Four-week-old plants were inoculated with 1×10^5 colony forming units (CFU) ml^{-1}, and bacterial counts per area of leaf plotted on a log scale at days 0, 2, and 4. Error bars represent SD of the mean of three samples and the experiment is representative of three independent replicates.

(B) Q-PCR quantification of *PR1* mRNA levels in Ws-0 (gray), *atg7* (black) or *atg9* (white) 4 and 8 hr after inoculation with avirulent *Pst* DC3000 (*AvrRpm1*) or (*AvrRps4*). Values are expressed in arbitrary units (as fold-increase of non-infected leaves) and corrected by normalization to an ubiquitin standard.

To verify this finding, we inoculated *atg7* and *atg9* mutants with an avirulent isolate (Noco2) of the oomycete *Hyaloperonospora arabidopsidis.* Recognition of Noco2 by the TIR-NB-LRR *RPP1* *R* gene leads to EDS1-dependent HR cell death 24 hr after inoculation (Parker et al., 1996). Accordingly, microscopic analysis of Ws-0 wild-type leaves stained with trypan blue to detect dead cells showed HR cell death of individual mesophyll cells penetrated by the oomycete 24 hr after inoculation (Figure 2C). This contrasted with *atg7*, in which there was a dramatic suppression of cell death ($p < 0.05$, Figure 2C). Cell death in *atg9* was also significantly suppressed ($p < 0.05$), but not to the extent as in *atg7* (Figure 2C). Collectively, these data indicate that autophagy may have a death promoting function in some plant-pathogen *R-Avr* gene interactions.

Autophagic Components Are Dispensable for Induced Resistance

Since autophagy was induced upon infection with *Pto* DC3000 expressing *AvrRps4* or *AvrRpm1*, the disease susceptibility of *atg7* and *atg9* mutants was examined. Time-course assays revealed that, after 2 days, growth of *Pto* DC3000 (*AvrRpm1*) or (*AvrRps4*) in *atg7* was up to 10-fold higher than growth in wild-type Ws-0 (Figure 3A). However, 4 days after challenge, bacterial levels had decreased in the autophagic mutants with the same magnitude as observed in wild-type plants (Figure 3A) and the

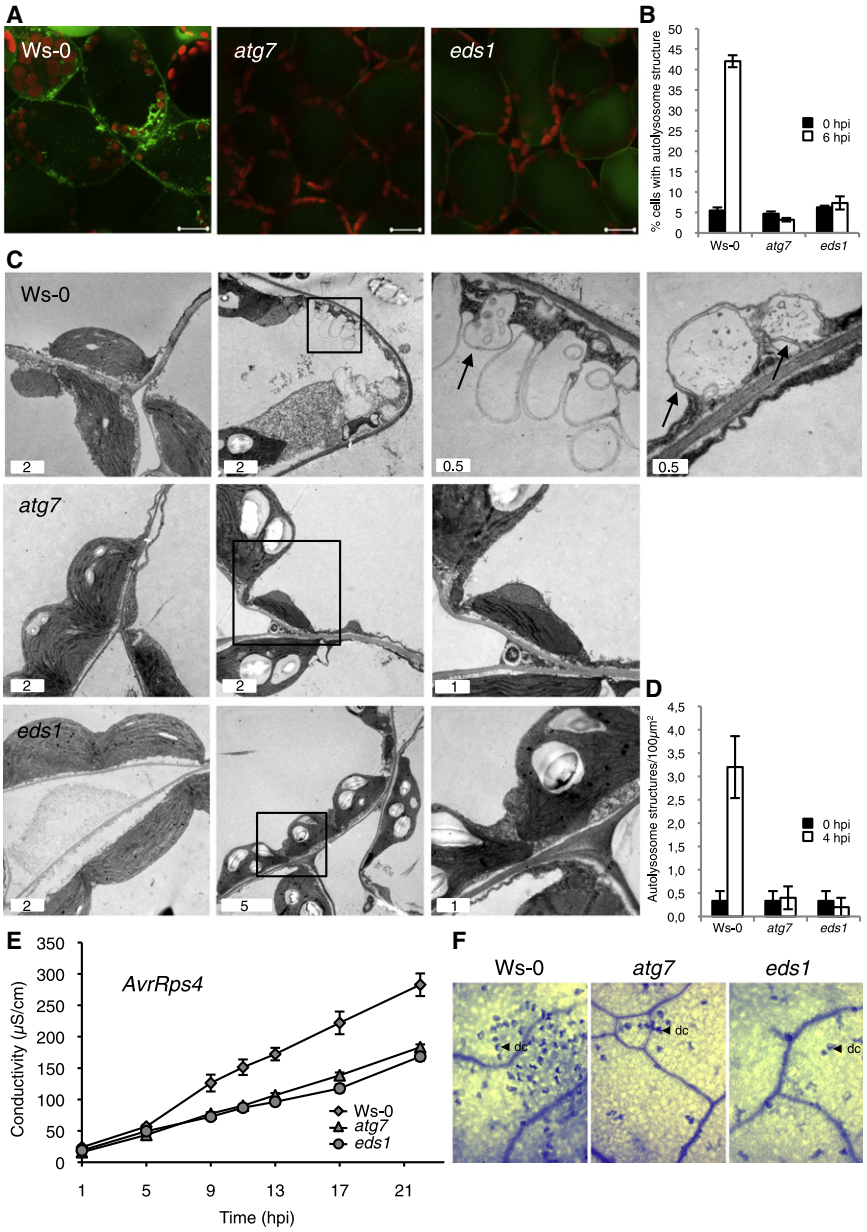

Figure 4. Mediation of RPS4-Conditioned Autophagic Cell Death via EDS1

(A) LysoTracker Green (LTG) staining of autolysosomal-like structures in leaves of Ws-0, *atg7* and *eds1* at 6 hr after infection with *Pto* DC3000 (*AvrRps4*). LTG-derived green fluorescence is superimposed with chlorophyll-specific red fluorescence. The scale bars represent 20 μm.

(B) Quantitation of cells with autolysosomal-like structures observed in LTG-stained tissue before and 6 hr after infection. Mean and standard error (SE) were calculated from three LTG-stained leaves per time point, and similar results obtained in three independent experiments with roughly 150 investigated cells per time point.

(C) Representative TEM images of the cytoplasm in mesophyll cells of Ws-0 (top), *atg7* (middle), and *eds1* (bottom) leaves before (left column) and 4 hr after infection with *Pto* DC3000 (*AvrRps4*). Boxes indicate areas enlarged in images presented in the right column. Additional image in wild-type shows an example of autophagosomal-like vesicles (arrows) in wild-type that are absent in *atg7* and *eds1* leaves. Scale bars represent the indicated numbers in μm.

(D) Quantitation of autolysosome/autophagosome structures observed in TEM images of mesophyll cells in Ws-0, *atg7* and *eds1* before and 4 hr after infection. Mean and standard error (SE) were calculated from 10 independent areas of 100 μm^2.

(E) Ion leakage measurements of leaves from wild-type, *atg7* and *eds1* after infection with *Pto* DC3000 (*AvrRps4*). Mean and standard error (SE) were calculated from four disks per treatment, with three replicates within an experiment.

(F) Lactophenol-trypan blue staining of dead cells (dc) in leaves (10× magnification) from Ws-0, *atg7*, and *eds1* plants 16 hr after infection with *Pto* DC3000 (*AvrRps4*).

AvrRps4 Activation of RPS4 Triggers Autophagy via EDS1

Since cell death provoked by *AvrRps4* is suppressed by mutations in autophagy genes, it is possible that RPS4 requires EDS1 to induce autophagy. We therefore infected *eds1* and *atg7* mutants with *Pto* DC3000 (*AvrRps4*) and tested for autophagic activity using LysoTracker Green staining. Again, this revealed a marked accumulation of autolysosomal-like structures in the cytoplasm of Ws-0 cells 6 hr post infection. In contrast, only few autolysosomal-like structures were observed in the cytoplasm of cells from *eds1* mutants that appeared indistinguishable from cells of *atg7* (Figures 4A and 4B). This observation was supported by transmission electron microscopic examination of infected leaves. Autophagosomal-like vesicles could be observed already 4 hr post infection in the cytoplasm of Ws-0 cells, but not in *atg7* and *eds1* (Figures 4C and 4D). In line with these observations, GFP-ATG8 mediated labeling of autophagosomal-like structures was absent from *Pto* DC3000 (*AvrRps4*) infected leaves in *eds1* (Figure S4). This prompted us to compare the level of cell death

defense marker *PR1* accumulated in both autophagic mutants to similar levels as in wild-type Ws-0 (Figure 3B). Thus, *atg7* and *atg9* mutants are compromised in early restriction of bacterial growth, but retain the capacity to induce other defense responses. However, knockdown of *BECLIN1/ATG6* leads to enhanced disease susceptibility, suggesting that autophagy contributes to basal defense responses (Patel and Dinesh-Kumar, 2008). In line with this notion, *atg7* mutants supported increased growth of virulent *Pto* DC3000 as well as of the virulent Emwa isolate of *H. arabidopsidis* (Figure S3). It is important to note, that we did not observe autophagy induction upon virulent *Pto* DC3000 infections during the first 6 hr post infection (Figure 1A), but we cannot exclude that autophagy might become activated, either at weaker levels or at later stages upon virulent infection.

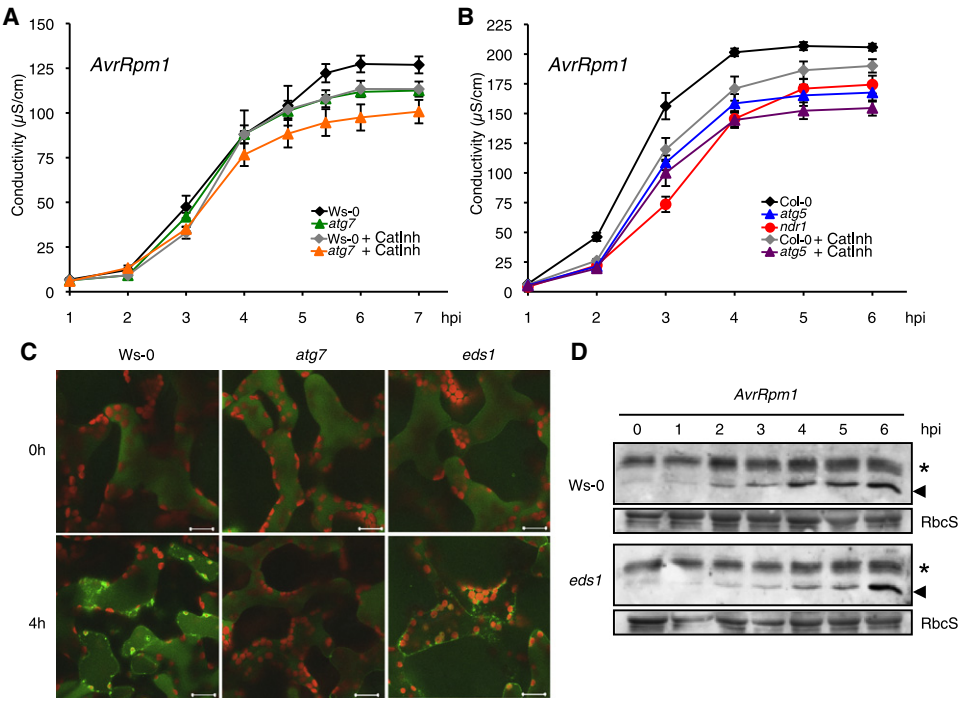

Figure 5. Involvement of Autophagy and Cathepsins in RPM1-Conditioned HR Cell Death

(A) Ion leakage assay after *Pto* DC3000 (*AvrRpm1*) infection of Ws-0 and *atg7* plants with or without cathepsin inhibitors (CatInh). Mean and standard error (SE) were calculated from four disks per treatment with three replicates within an experiment.

(B) Ion leakage assay after *Pto* DC3000 (*AvrRpm1*) infection of Col-0 and *atg5* plants with or without cathepsin inhibitors in comparison to *ndr1*. Mean and standard error (SE) were calculated from four disks per treatment with four replicates within an experiment.

(C) LysoTracker Green (LTG) staining indicative of autolysosomal structures in leaves of Ws-0, *atg7* and *eds1* at 0 and 4 hr after infection with *Pto* DC3000 (*AvrRpm1*). LTG-derived green fluorescence is superimposed with red fluorescence of chlorophyll. The scale bars represent 20 µm.

(D) Immunoblot analysis of ATG8 accumulation and modification in Ws-0 and *eds1* plants upon infection with *Pto* DC3000 (*AvrRpm1*). Total proteins were extracted from leaf tissue sampled at the indicated times and probed by Western blotting with anti-ATG8a antiserum. Unmodified forms of ATG8 are marked by an asterisk and faster migrating bands indicative of ATG8 modification are indicated by arrowheads. Crossreacting Rubisco large subunit (RbcS) served as loading controls. Upper panel is the same as in Figure 1B for comparison.

suppression between *eds1* and *atg7* infected with *Pto* DC3000 (*AvrRps4*). In Ws-0, an increase in conductance was apparent by 9 hr (Figure 4E). As observed previously, this increase was considerably suppressed in the *atg7* mutant. Remarkably, we did not observe a significant difference in electrolyte leakage between *atg7* and *eds1* (Figure 4E). This was supported by similar trypan blue stainings of *atg7* and *eds1* infected with Noco2 isolates of *H. arabidopsidis* (Figure 2C) and infections with *Pto* DC3000 (*AvrRps4*) (Figure 4F). Thus, EDS1 seems to be required for early induction of autophagy via RPS4, and *eds1* and *atg7* suppress *AvrRps4*-induced cell death to comparable levels.

Autophagy and Cathepsins Promote RPM1-Triggered Cell Death

The observation that autophagy is induced by *Pto* DC3000 (*AvrRpm1*) could indicate that autophagy is, at least in part, involved in RPM1-mediated PCD execution. To analyze the possibility that the contribution of autophagy is masked by (an)other cell death pathway(s) in RPM1-mediated PCD execution, we set out to block another PCD mechanism in the autophagy deficient background. One such pathway may involve cathepsin B which was recently demonstrated by experiments with inhibitors and antisense to be required for cell death in *N. benthamiana* triggered by *Phytophthora infestans* (Gilroy et al., 2007). In our *Arabidopsis* system, cathepsin inhibitor treatments resulted only in a slight but not significant reduction of cell death upon infection with *Pto* DC3000 (*AvrRpm1*) in the Ws-0 wild-type, and this reduction was comparable to the effect of autophagy deficiency in *atg7* (Figure 5A). However, the use of cathepsin inhibitors on *atg7* mutants revealed an additive effect, and resulted in considerable reduction of cell death compared to wild-type ($p < 0.05$ at 6 and 7 hpi). To analyze the biological relevance of this effect, we compared the level of cell death suppression to the signaling mutant *ndr1* which is partially compromised in RPM1-conditioned resistance and HR cell death (Aarts et al., 1998). Because the *ndr1-1* knockout allele is in the Col-0 background, we extended our studies and included an *atg5* loss-of-function mutant in the same ecotype (Thompson et al., 2005). As observed before, *Pto* DC3000 (*AvrRpm1*)-triggered cell death was comparably reduced by autophagy deficiency and cathepsin inhibition in relation to the wild-type control (Col-0). However, an additive effect leading to significant suppression of RPM1-conditioned cell death ($p < 0.05$ at 4-6 hpi) could be observed after cathepsin inhibitor treatment of *atg5* plants, which reached levels resembling

ndr1 (Figure 5B). These findings were further substantiated with an additional *atg7* knockout allele (*atg7-2*) in the Col-0 background (Figure S5). In addition, cell death suppression by autophagy deficiency in combination with cathepsin inhibitor treatment became more evident under conditions with increased day length similar to those used by Patel and Dinesh-Kumar (2008) (Figure S6A). Collectively, these data indicate that RPM1 engages multiple cell death pathways including at least one that depends on autophagy and another that requires lysosomal cathepsins. Since RPM1-mediated defense responses are only partially NDR1-dependent and known to also involve EDS1 (Bartsch et al., 2006), we speculated that autophagy might be induced via EDS1 upon infection with *Pto* DC3000 (*AvrRpm1*). As revealed by LysoTracker Green staining and the processing of ATG8, autophagic like activity could still be induced by *Pto* DC3000 (*AvrRpm1*) in *eds1* mutants (Figures 5C and 5D). We therefore examined the cell death response of *eds1* provoked with *Pto* DC3000 (*AvrRpm1*). Surprisingly, *eds1* plants exhibited accelerated cell death compared to wild-type (Figure S7).

RPS2-Conditioned Cell Death via NDR1 Is Autophagy-Independent

RPM1 belongs to the CC-NB-LRR class of innate immune receptors, and the avirulence factor AvrB activates defense responses via both RPM1 and TAO1, a TIR-NB-LRR protein (Eitas et al., 2008). It is therefore possible that the strong activation of cell death and defense responses upon AvrRpm1 recognition is because this avirulence factor engages RPM1 and other receptors including a TIR-NB-LRR protein that subsequently induces autophagy. To analyze the role of autophagy in HR PCD responses solely conditioned by the CC-NB-LRR type receptor pathway via the signaling component NDR1, we infected *Arabidopsis* with *Pto* DC3000 harboring AvrRpt2. This avirulence factor is recognized by the CC-NB-LRR type R protein RPS2 and triggers hypersensitive cell death which, in contrast to RPM1-conditioned HR PCD, is strictly NDR1-dependent (Mackey et al., 2003). Interestingly, we observed only weak accumulation of autophagic like activity by LysoTracker Green staining in wild-type Col-0 leaves. Even 6 hr post infection, when autophagy is strongly induced in plants infected with *Pto* DC3000 (*AvrRpm1* or *AvrRps4*), only minor differences could be observed between uninfected and infected plants (Figure 6A). This was substantiated by the observation that autophagic activity could not be induced by *Pto* DC3000 (*AvrRpt2*) in *ndr1* (Figure 6A). In addition, inoculation of *atg5* and *atg7* mutants with *Pto* DC3000 (*AvrRpt2*) did not result in significant reduction in electrolyte leakage compared to wild-type (Figure 6B), cathepsin inhibitors had no measurable effect (Figure 6C), and cell death suppression was only observed for *ndr1* (Figures 6B and 6C). However, multiple experiments indicated a trend in which the *atg* mutants had slightly more leakage in the initial phases of HR execution (Figure 6B), which proved to be significant ($p < 0.05$ at 7 hpi) for *atg7* irrespective of cathepsin treatment (Figure 6C). This raised the question whether autophagy functions as a negative cell death regulator under *Pto* DC3000 (*AvrRpt2*) infections. Nonetheless, as seen for other avirulent bacterial infections (Figure S1), lesions in response to *Pto* DC3000 (*AvrRpt2*) infection were contained in *atg* mutants (Figure 6D).

Since *Pto* DC3000 delivers approximately 30 effectors into the host (Chang et al., 2005), we asked whether the different forms of R-protein mediated cell death studied are elicited exclusively by the perception of AvrRps4, AvrRpm1 or AvrRpt2 inside the plant cell. Therefore, we employed a genetically modified, nonpathogenic *Pseudomonas fluorescens* (Pf0-1) strain to deliver only single avirulence factors into *Arabidopsis* leaves (W. Thomas, personal communication). This demonstrated that all three avirulence effectors induced HR cell death independently of other bacterial effectors. In addition, AvrRps4- and AvrRpm1-induced cell death was suppressed to similar levels in autophagy deficient mutants as seen with the avirulent *Pto* DC3000 strains, whereas AvrRpt2-triggered cell death proved to be independent of autophagy (Figure S8).

DISCUSSION

Controversy Surrounding the Roles of Autophagy in Plant Cell Death

The genetic evidence presented here for a prodeath function of autophagy during pathogen-triggered HR is in contrast to a previously proposed model. Liu et al. (2005) first reported the requirement for autophagic components, including *ATG7* and *BECLIN1/ATG6*, to negatively regulate HR-associated PCD in tobacco plants triggered by viral infection and pathogen elicitors. In line with this finding, unrestricted cell death was also observed in *BECLIN1/ATG6* silenced *Arabidopsis* infected with *Pto* DC3000 harboring *AvrRpm1* (Patel and Dinesh-Kumar, 2008). Although their observation of rapid autophagy activation upon avirulent pathogen infection proved to be robust (Figure 1), we did not detect spreading of disease- and HR-related PCD in autophagy-deficient knockout mutants using the same bacterial strain *Pto* DC3000 (*AvrRpm1*) under comparable growth conditions (Figures S1A–S1C and S6B).

This apparent discrepancy between prosurvival and prodeath functions of autophagic components in *Arabidopsis* and other plants may indicate differences in the efficiency or specificity of knockout or antisense plants to block specific processes. On the other hand, plants apparently employ several mechanisms to execute cell death, as reflected in the differences noted above for cell death following inoculation with *Pto* DC3000 harboring *AvrRps4*, *AvrRpm1* or *AvrRpt2*. It has been demonstrated that knockout of *ATG6/Beclin* in *Caenorhabditis elegans* leads to inappropriate activation of apoptosis (Takacs-Vellai et al., 2005). Similarly, inhibition of macroautophagy by silencing components such as *ATG5*, *ATG6/Beclin1-1*, *ATG10* or *ATG12* in mammalian cells triggers apoptosis upon nutrient depletion (Boya et al., 2005). This suggests that *Arabidopsis BECLIN1/ATG6,* as in animals, affects several pro-death pathways such that its antisense downregulation leads to inappropriate activation of early senescence-related cell death that is accelerated upon infection. In this context, we note that our observations include a quantitative assay performed during the time-course of HR execution. Such HR-triggered cell death develops within hours, in contrast to the spreading lesions in *BECLIN1/ATG6* silenced plants which occur after several days (Patel and Dinesh-Kumar, 2008). Nonetheless, our results also suggest that autophagy has a cytoprotective role in HR execution, because RPS2 conditioned cell

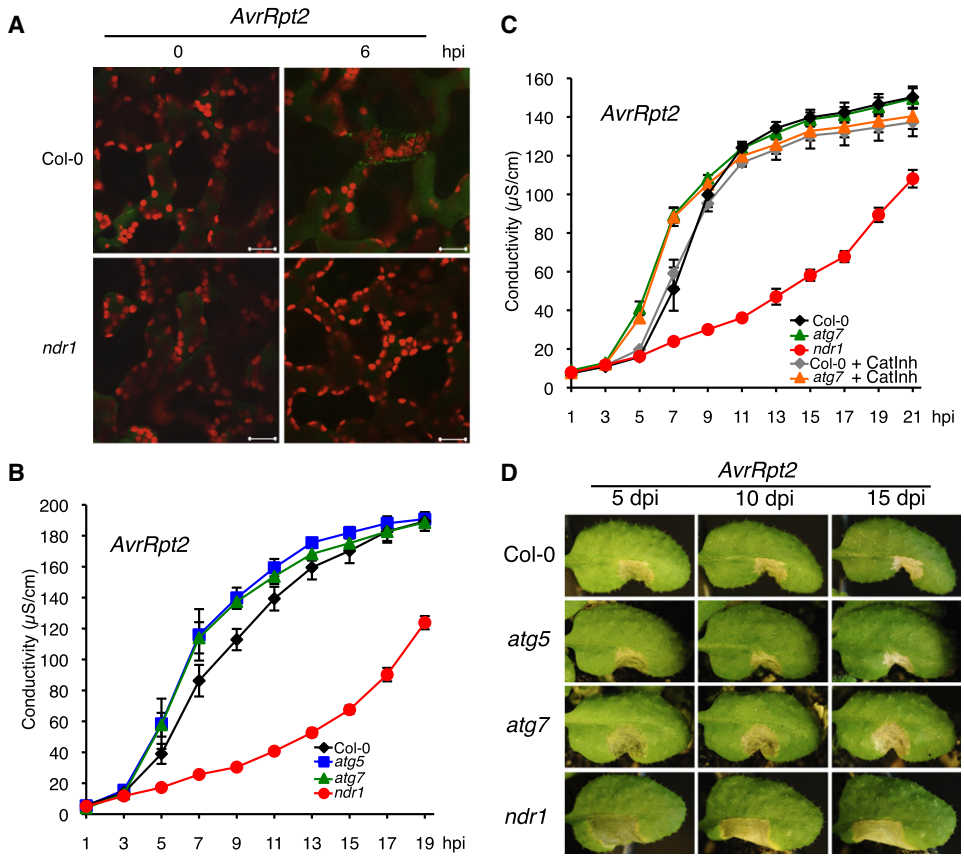

Figure 6. RPS2-Conditioned HR Cell Death Does Not Engage Autophagy Components and Cathepsins, and Remains Restricted in *atg* Mutants

(A) LysoTracker Green (LTG) staining in Col-0 and *ndr1* plants at 0 and 6 hr after infection with *Pto* DC3000 expressing *AvrRpt2*. LTG-specific fluorescence is superimposed with chlorophyll-derived red fluorescence and indicates only weak autophagy activation upon *Pto* DC3000 (*AvrRpt2*) infection.

(B) Ion leakage assay after *Pto* DC3000 (*AvrRpt2*) infection of autophagy deficient *atg5* and *atg7* mutants in comparison to Col-0 and *ndr1* control lines. Mean and standard error (SE) were calculated from four disks per treatment with four replicates within an experiment.

(C) Ion leakage assay after *Pto* DC3000 (*AvrRpt2*) infection of Col-0 and *atg7* plants with and without cathepsin inhibitor (CatInh) in comparison to *ndr1*. Mean and standard error (SE) were calculated from four disks per treatment with four replicates within an experiment.

(D) *Pto* DC3000 (*AvrRpt2*) induced HR lesions are contained in *atg5* and *atg7* mutants. Representative images of wild-type (Col-0), *atg5, atg7* and *ndr1* plants 5, 10, and 15 days after local infection with avirulent *Pto* DC3000 harboring *AvrRpt2*.

death initially appeared slightly faster in *atg* mutants (Figures 6B and 6C). Nevertheless, lesions induced by *Pto* DC3000 (*AvrRpt2*) do not spread beyond infection sites, suggesting that a given interplay between autophagy and other cell death pathways only affects primary infection sites in this system. In addition, our observation that accelerated cell death occurs in the presence of increased autophagic activity in *eds1* (Figure S7) indicates that disruption of a number of different genes can cause this symptomatic phenomenon.

Although autophagy has been associated with both cell survival and cell death in eukaryotes, the role of autophagy in cell death execution is still debated (Kroemer and Levine, 2008). Nevertheless, unequivocal evidence was recently presented that autophagy participates in physiologically relevant cell death in *Drosophila* and necrotic PCD in *C. elegans* (Berry and Baehrecke, 2007; Samara et al., 2008). Since autophagy is required for cellular homeostasis in response to many physiological cues, it is not surprising that some controversy surrounds its functions. For example, autophagy is required to dampen the deleterious effects upon ER stress (Bernales et al., 2006). It is therefore tempting to suggest that many stress responses that activate cell death pathways also trigger the unfolded protein response (UPR). Therefore, in situations where autophagy is required for both processes, the final outcome will ultimately be death when examined in *atg* mutants. Under some circumstances, such a death process may even be faster if the inducer first activates a strong UPR and cells are unable to cope with the situation.

Multiple Routes to Cell Death in Plant Pathogen Interactions

Our data further suggest that the RPS4-conditioned autophagy response depends on the EDS1 regulatory node (Figure 4). While this implies that EDS1 is a general regulator of autophagy, Bartsch et al. (2006) showed that induction of pathogen-responsive

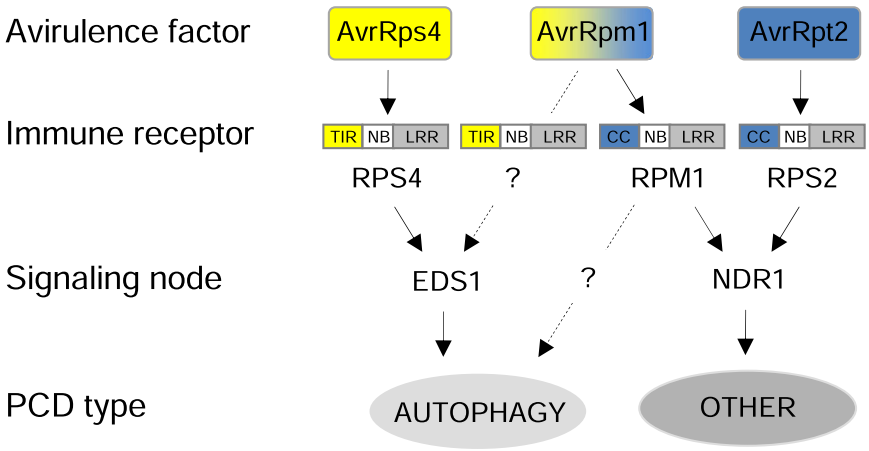

Figure 7. A Model for the Induction of Autophagic Cell Death upon TIR-NB-LRR and/or CC-NB-LRR Immune Receptor Activation by Bacterial Avirulence Factors

RPS4-conditioned HR cell death via the defense regulator EDS1 involves the autophagy machinery. Autophagic cell death is also engaged in RPM1-triggered cell death in parallel with other types of PCD that involve cathepsins. *AvrRpm1*-triggered HR may include activation of an as yet unidentified TIR-NB-LRR immune receptor to induce autophagy via EDS1, but may also involve an EDS1-independent pathway for autophagy activation. In contrast to RPS4- and RPM1-conditioned HR cell death, RPS2-triggered PCD is fully mediated by NDR1 and independent of both autophagy and cathepsins.

autophagy genes is specifically compromised in *eds1* compared to wild-type (Ws-0) upon challenge with *Pto* DC3000 *(AvrRps4)*, but not with *Pto* DC3000 (*AvrRpm1*) (Figure S9). In addition, we observed EDS1-independent induction of autophagy when plants were challenged with *Pto* DC3000 harboring *AvrRpm1* (Figures 5C and 5D). Thus, EDS1 does not appear to function as a general regulator of the autophagy pathway. A recent study by Wirthmueller et al. (2007) rather supports the hypothesis that EDS1 links activated and nuclear-localized RPS4 to autophagy and other responses as part of an overall transcriptional defense response in the nucleus.

Our study indicates that other death types operate in *Arabidopsis*. That *Pto* DC3000 (*AvrRpm1*) HR cell death is partially but significantly suppressed in *atg* mutants treated with cathepsin inhibitors (Figures 5B, S5, and S6), but not upon *Pto* DC3000 (*AvrRpt2*) infection (Figure 6C), supports such a model. Other cell death routes are likely to be induced via NDR1 because *AvrRpm1* triggered cell death was only suppressed to levels observed for *ndr1*, and we could not suppress NDR1-dependent cell death. These pathways could include vacuolar proteases or metacaspases (Hatsugai et al., 2004; He et al., 2008), but how these enzymes relate to autophagy is currently unknown.

Models for Autophagic Cell Death in Plant Innate Immunity

The data presented here do not resolve to what extent autophagy is required to facilitate signal transduction leading to death, or to more directly effectuate cell death. Resolution of this issue will require the development of assays of the relative levels over time of plant immune receptor signaling elicited by pathogen avirulence factors in wild-type and *atg* mutants. Nonetheless, the results presented here may be included in a simplistic model (Figure 7) in which autophagy is induced upon activation of the TIR-NB-LRR immune receptor RPS4. Because we did not observe autophagic activity in *AvrRps4* challenged *eds1* mutants, the genetics of this system indicate that EDS1 acts upstream of autophagy in RPS4 triggered PCD. In another scenario, the CC-NB-LRR receptor RPM1 also recruits autophagy for cellular destruction. However, in this case other pathways to cell demise are also activated and cell death is executed rapidly. We suggest that the activation of RPM1 by AvrRpm1 may include TIR-NB-LRR activation as well, but because AvrRpm1 also results in autophagic activation in *eds1* mutants, RPM1 probably activates autophagy by other means. Thus, both RPS2 and RPM1 trigger NDR1-dependent cell death which is apparently independent of autophagic execution. However, we cannot exclude that a CC-NB-LRR receptor(s) may induce a strong ER stress, via NDR1, that could mask an autophagic contribution to cell death.

In conclusion, we present a primary example of a cell death pathway operating in plants that involves autophagic mechanisms. We provide evidence that an(other) cell death pathway(s) can be invoked in plants by different pathogens. This raises questions of how or why similar resistance genes engage different execution pathways. An explanation may be that the defense machinery maintains more than one pathway to enable different types of cells to commit suicide in response to different stimuli or developmental cues. By keeping different death pathways linked to different innate immune receptors, other principal downstream signaling components may be shared between the pathways. Thus, *eds1* and *ndr1* mutants exhibit cell death when infected with pathogens expressing effectors recognized by receptors that require EDS1 or NDR1 for signaling, Similarly, cell death triggered by avirulent pathogens is only delayed in *atg* mutants, and the kind of quantitative assays used here are needed to identify the contribution of the individual pathways.

EXPERIMENTAL PROCEDURES

Plant Material and Growth Conditions

Arabidopsis eds1-1 and *ndr1-1* mutants, as well as autophagy knockout lines *atg7-1, atg9-1* and *atg5-1* have been described (Aarts et al., 1998; Doelling et al., 2002; Thompson et al., 2005). The *atg7-2* mutant (GK-655B06) was obtained from NASC (http://arabidopsis.info; #N462802) and homozygous insertion lines were verified with primers specific for the T-DNA left border in combination with ATG7 specific primers (Table S1). Plants were soil grown in environmental chambers under 8 hr light regime (150 $\mu E/m^2s$) at 21°C and 70% relative humidity.

Pathogen Assays and Inhibitor Treatment

Arabidopsis infections with *H. arabidopsidis* isolate Noco2 were performed using 5 × 10^5 conidia ml^{-1} and monitored by lactophenol-trypan blue staining

as described previously (Parker et al., 1996, 1997). Bacterial ion leakage assays following syringe-infiltration of virulent or avirulent *Pseudomonas syringae* pv. tomato (*Pto*) DC3000 strains were performed after Mackey et al. (2003) with 2×10^8 CFU ml^{-1}. Infiltration of leaf areas for assessment of spreading HR cell death used 2×10^7 CFU ml^{-1} as described by Patel and Dinesh-Kumar (2008). For inhibitor studies, bacterial suspensions were pressure infiltrated with or without 1 mM cathepsin inhibitor (cathepsin B, S, and L inhibitor, Z-FGNHO-Bz; Calbiochem, Merck Biosciences) prepared as 100 mM stock solution in 1% DMSO. Control treatments without inhibitor were with 1% DMSO.

Confocal and Electron Microscopy

Agrobacterium tumefaciens strain GV3101 harboring the binary plasmids GFP-ATG8i or GFP-ATG8e (Yoshimoto et al., 2004) were co-infiltrated at an optical density of 1.0:1.0 (600 nm) into the abaxial air space of 3-week-old plants. Two days after agro-infiltration, leaves were infected with bacteria as described above for the ion leakage assays and visualized with a Zeiss LSM510 confocal microscope using excitation light of 488 nm and emission filters of BP505-550nm and LP650nm to allow detection of GFP or chlorophyll-derived red fluorescence, respectively. Images were superimposed with Zeiss LSM Version 3.2 software.

LysoTracker Green (LTG) fluorescence indicative of autophagy activity (Moriyasu et al., 2003; Liu et al., 2005) was detected by confocal microscopy with the same settings as for GFP fluorescence. Leaves were vacuum-infiltrated with 1 μM LTG (DND-26, Invitrogen Molecular Probes, Eugene, Oregon, US) at time points after bacterial infection and kept for an additional hour in darkness before visualization. Quantitation of LTG stained autophagosomal-like structures followed the method described in Liu et al. (2005).

For transmission electron microscopy (TEM), middle areas of leaves were cut into transverse sections less than 1 mm wide and fixed in 2.0% paraformaldehyde and 2.5% glutaraldehyde in 0.1 M phosphate buffer (pH 7.0) overnight at 5°C. After washing in buffer, sections were postfixed for 2 hr at room temperature in buffered 1% OsO_4, then washed in buffer and water and dehydrated in a graded series of acetone before infiltration with Spurr's embedding mixture (Bozzola and Russell, 1999). 1 mm^2 areas of leaf lamina lateral to the mid-vein were then embedded, sectioned (50–100 nm) with a diamond knife on a Reichert-Jung Super Nova ultra-microtome, collected on slot-grids with formvar film, and stretched by chloroform vapor. Sections were contrasted with uranyl acetate and lead citrate and examined in a Jeol 1010CX transmission electron microscope with a Gatan digital camera. Quantitation of autolysosome/autophagosome structures in TEM sections was done as described in Liu et al. (2005).

Immunoblot analysis

Total proteins of leaf material were extracted with 50 mM Tris (pH 7.0), 150 mM NaCl, 150 mM EDTA, 1× Protease inhibitor cocktail (Roche, Mannheim, Germany) and subjected to SDS-PAGE with 6 M urea. Western blotting with α-ATG8a antiserum (kindly provided by Y. Ohsumi, Okazaki, Japan) followed standard procedures (for details see Supplemental Experimental Procedures).

Quantitative (Q) RT-PCR Analysis

Total RNA was extracted using the RNAgents Total RNA isolation system (Promega, Madison, WI). Q-PCR of *PR1* expression was performed using the SYBR Green kit (Applied Biosystems, Foster City, CA) with ubiquitin (*UBQ10*) expression as standard reference (see Supplemental Experimental Procedures for details) .

Statistical Analysis

Statistical analyses were performed with an ANOVA with post hoc Tukey's test or student's t test. Significance was accepted at the level of $p < 0.05$.

SUPPLEMENTAL DATA

Supplemental Data include Supplemental Experimental Procedures, Supplemental References, nine figures, and one table and can be found with this article online at http://www.cell.com/supplemental/S0092-8674(09)00250-5.

ACKNOWLEDGMENTS

We thank Suksawad Vongvisuttikun, Henriette Larsen, and Lis Munk Frederiksen for technical assistance. We also thank Yoshinori Ohsumi (National Institute for Basic Biology, Okazaki, Japan) and Kohki Yoshimoto (RIKEN Plant Science Center, Yokohama, Japan) for carefully reading versions of this manuscript and providing binary plasmids carrying GFP-ATG8s as well as seeds of *atg9* and *atg4a/b*. We are grateful to R. Vierstra (University of Wisconsin, Madison, WI) for providing seeds of *atg7* and *atg5*. Finally, we thank J. Chang (Oregon State University, Corvallis, OR) for providing modified Pf0-1 strains. This work was funded by grants to J.M. from the Danish Cancer Society (DP03048) and Research Council (274-06-0460, 272-06-0049), and the European Union (LSHG-CT-2004-511983) as well as to M.P. (23-02-0101) and D.H. (23-04-0143) from the Danish Agricultural Research Council.

Received: September 12, 2008
Revised: December 23, 2008
Accepted: February 12, 2009
Published: May 14, 2009

REFERENCES

Aarts, N., Metz, M., Holub, E., Staskawicz, B.J., Daniels, M.J., and Parker, J.E. (1998). Different requirements for EDS1 and NDR1 by disease resistance genes define at least two R gene-mediated signaling pathways in Arabidopsis. Proc. Natl. Acad. Sci. USA *95*, 10306–10311.

Abramovitch, R.B., Anderson, J.C., and Martin, G.B. (2006). Bacterial elicitation and evasion of plant innate immunity. Nat. Rev. Mol. Cell Biol. *7*, 601–611.

Bartsch, M., Gobbato, E., Bednarek, P., Debey, S., Schultze, J.L., Bautor, J., and Parker, J.E. (2006). Salicylic acid-independent ENHANCED Dros. Inf. Serv. EASE SUSCEPTIBILITY1 signaling in Arabidopsis immunity and cell death is regulated by the monooxygenase FMO1 and the Nudix hydrolase NUDT7. Plant Cell *18*, 1038–1051.

Bassham, D.C., Laporte, M., Marty, F., Moriyasu, Y., Ohsumi, Y., Olsen, L.J., and Yoshimoto, K. (2006). Autophagy in development and stress responses of plants. Autophagy *2*, 2–11.

Bent, A.F., and Mackey, D. (2007). Elicitors, effectors, and R genes: the new paradigm and a lifetime supply of questions. Annu. Rev. Phytopathol. *45*, 399–436.

Bernales, S., McDonald, K.L., and Walter, P. (2006). Autophagy counterbalances endoplasmic reticulum expansion during the unfolded protein response. PLoS Biol. *4*, e423. 10.1371/journal.pbio.0040423.

Berry, D.L., and Baehrecke, E.H. (2007). Growth arrest and autophagy are required for salivary gland cell degradation in Drosophila. Cell *131*, 1137–1148.

Boya, P., Gonzalez-Polo, R.A., Casares, N., Perfettini, J.L., Dessen, P., Larochette, N., Metivier, D., Meley, D., Souquere, S., Yoshimori, T., et al. (2005). Inhibition of macroautophagy triggers apoptosis. Mol. Cell. Biol. *25*, 1025–1040.

Bozzola, J.J., and Russell, L.D. (1999). Electron Microscopy; Principles and Techniques for Biologists. 2 (Boston, USA: Jones and Bartlett).

Chang, J.H., Urbach, J.M., Law, T.F., Arnold, L.W., Hu, A., Gombar, S., Grant, S.R., Ausubel, F.M., and Dangl, J.L. (2005). A high-throughput, near-saturating screen for type III effector genes from Pseudomonas syringae. Proc. Natl. Acad. Sci. USA *102*, 2549–2554.

Dangl, J.L., and Jones, J.D. (2001). Plant pathogens and integrated defence responses to infection. Nature *411*, 826–833.

Doelling, J.H., Walker, J.M., Friedman, E.M., Thompson, A.R., and Vierstra, R.D. (2002). The APG8/12-activating enzyme APG7 is required for proper nutrient recycling and senescence in Arabidopsis thaliana. J. Biol. Chem. *277*, 33105–33114.

Edinger, A.L., and Thompson, C.B. (2004). Death by design: apoptosis, necrosis and autophagy. Curr. Opin. Cell Biol. *16*, 663–669.

Eitas, T.K., Nimchuk, Z.L., and Dangl, J.L. (2008). Arabidopsis TAO1 is a TIR-NB-LRR protein that contributes to disease resistance induced by the Pseudomonas syringae effector AvrB. Proc. Natl. Acad. Sci. USA *105*, 6475–6480.

Geng, J., and Klionsky, D.J. (2008). The Atg8 and Atg12 ubiquitin-like conjugation systems in macroautophagy. 'Protein modifications: beyond the usual suspects' review series. EMBO Rep. *9*, 859–864.

Gilroy, E.M., Hein, I., van der Hoorn, R., Boevink, P.C., Venter, E., McLellan, H., Kaffarnik, F., Hrubikova, K., Shaw, J., Holeva, M., et al. (2007). Involvement of cathepsin B in the plant disease resistance hypersensitive response. Plant J. *52*, 1–13.

Guicciardi, M.E., Leist, M., and Gores, G.J. (2004). Lysosomes in cell death. Oncogene *23*, 2881–2890.

Gutierrez, M.G., Master, S.S., Singh, S.B., Taylor, G.A., Colombo, M.I., and Deretic, V. (2004). Autophagy is a defense mechanism inhibiting BCG and Mycobacterium tuberculosis survival in infected macrophages. Cell *119*, 753–766.

Harrison-Lowe, N.J., and Olsen, L.J. (2008). Autophagy Protein 6 (ATG6) is Required for Pollen Germination in Arabidopsis thaliana. Autophagy *4*, 339–348.

Hatsugai, N., Kuroyanagi, M., Yamada, K., Meshi, T., Tsuda, S., Kondo, M., Nishimura, M., and Hara-Nishimura, I. (2004). A plant vacuolar protease, VPE, mediates virus-induced hypersensitive cell death. Science *305*, 855–858.

He, R., Drury, G.E., Rotari, V.I., Gordon, A., Willer, M., Farzaneh, T., Woltering, E.J., and Gallois, P. (2008). Metacaspase-8 modulates programmed cell death induced by ultraviolet light and H2O2 in Arabidopsis. J. Biol. Chem. *283*, 774–783.

Hofius, D., Tsitsigiannis, D.I., Jones, J.D., and Mundy, J. (2007). Inducible cell death in plant immunity. Semin. Cancer Biol. *17*, 166–187.

Ichimura, Y., Imamura, Y., Emoto, K., Umeda, M., Noda, T., and Ohsumi, Y. (2004). In vivo and in vitro reconstitution of Atg8 conjugation essential for autophagy. J. Biol. Chem. *279*, 40584–40592.

Jones, J.D., and Dangl, J.L. (2006). The plant immune system. Nature *444*, 323–329.

Klionsky, D.J., Abeliovich, H., Agostinis, P., Agrawal, D.K., Aliev, G., Askew, D.S., Baba, M., Baehrecke, E.H., Bahr, B.A., Ballabio, A., et al. (2008). Guidelines for the use and interpretation of assays for monitoring autophagy in higher eukaryotes. Autophagy *4*, 151–175.

Kroemer, G., and Levine, B. (2008). Autophagic cell death: the story of a misnomer. Nat. Rev. Mol. Cell Biol. *9*, 1004–1010.

Lam, E., Kato, N., and Lawton, M. (2001). Programmed cell death, mitochondria and the plant hypersensitive response. Nature *411*, 848–853.

Lam, E. (2004). Controlled cell death, plant survival and development. Nat. Rev. Mol. Cell Biol. *5*, 305–315.

Levine, B., and Klionsky, D.J. (2004). Development by self-digestion: molecular mechanisms and biological functions of autophagy. Dev. Cell *6*, 463–477.

Liu, Y., Schiff, M., Czymmek, K., Talloczy, Z., Levine, B., and Dinesh-Kumar, S.P. (2005). Autophagy regulates programmed cell death during the plant innate immune response. Cell *121*, 567–577.

Mackey, D., Belkhadir, Y., Alonso, J.M., Ecker, J.R., and Dangl, J.L. (2003). Arabidopsis RIN4 is a target of the type III virulence effector AvrRpt2 and modulates RPS2-mediated resistance. Cell *112*, 379–389.

Mizushima, N. (2007). Autophagy: process and function. Genes Dev. *21*, 2861–2873.

Moriyasu, Y., Hattori, M., Jauh, G.Y., and Rogers, J.C. (2003). Alpha tonoplast intrinsic protein is specifically associated with vacuole membrane involved in an autophagic process. Plant Cell Physiol. *44*, 795–802.

Nakagawa, I., Amano, A., Mizushima, N., Yamamoto, A., Yamaguchi, H., Kamimoto, T., Nara, A., Funao, J., Nakata, M., Tsuda, K., et al. (2004). Autophagy defends cells against invading group A Streptococcus. Science *306*, 1037–1040.

Nimchuk, Z., Eulgem, T., Holt, B.F., 3rd, and Dangl, J.L. (2003). Recognition and response in the plant immune system. Annu. Rev. Genet. *37*, 579–609.

Parker, J.E., Coleman, M.J., Szabo, V., Frost, L.N., Schmidt, R., van der Biezen, E.A., Moores, T., Dean, C., Daniels, M.J., and Jones, J.D. (1997). The Arabidopsis downy mildew resistance gene RPP5 shares similarity to the toll and interleukin-1 receptors with N and L6. Plant Cell *9*, 879–894.

Parker, J.E., Holub, E.B., Frost, L.N., Falk, A., Gunn, N.D., and Daniels, M.J. (1996). Characterization of eds1, a mutation in Arabidopsis suppressing resistance to Peronospora parasitica specified by several different RPP genes. Plant Cell *8*, 2033–2046.

Patel, S., and Dinesh-Kumar, S.P. (2008). Arabidopsis ATG6 is required to limit the pathogen-associated cell death response. Autophagy *4*, 20–27.

Samara, C., Syntichaki, P., and Tavernarakis, N. (2008). Autophagy is required for necrotic cell death in Caenorhabditis elegans. Cell Death Differ. *15*, 105–112.

Seay, M., Patel, S., and Dinesh-Kumar, S.P. (2006). Autophagy and plant innate immunity. Cell. Microbiol. *8*, 899–906.

Takacs-Vellai, K., Vellai, T., Puoti, A., Passannante, M., Wicky, C., Streit, A., Kovacs, A.L., and Muller, F. (2005). Inactivation of the autophagy gene bec-1 triggers apoptotic cell death in C. elegans. Curr. Biol. *15*, 1513–1517.

Thompson, A.R., Doelling, J.H., Suttangkakul, A., and Vierstra, R.D. (2005). Autophagic nutrient recycling in Arabidopsis directed by the ATG8 and ATG12 conjugation pathways. Plant Physiol. *138*, 2097–2110.

Vercammen, D., Declercq, W., Vandenabeele, P., and Van Breusegem, F. (2007). Are metacaspases caspases? J. Cell Biol. *179*, 375–380.

Wirthmueller, L., Zhang, Y., Jones, J.D., and Parker, J.E. (2007). Nuclear accumulation of the Arabidopsis immune receptor RPS4 is necessary for triggering EDS1-dependent defense. Curr. Biol. *17*, 2023–2029.

Woltering, E.J. (2004). Death proteases come alive. Trends Plant Sci. *9*, 469–472.

Yoshimoto, K., Hanaoka, H., Sato, S., Kato, T., Tabata, S., Noda, T., and Ohsumi, Y. (2004). Processing of ATG8s, ubiquitin-like proteins, and their deconjugation by ATG4s are essential for plant autophagy. Plant Cell *16*, 2967–2983.